Real-time wall conditioning through B powder injection in fusion devices

A. Bortolon[1], E. Gilson[1], R. Lunsford[1], R. Maingi[1], A. Nagy[1], A. Hyatt[2], T. Wilks[3], M. Fenstermacher[4], C. Samuell[4], J. Boedo[5], D. Rudakov[5], M. Shafer[6], A. Maan[7], D. Donovan[7], J. Duran[7], J. Ren[7], R. Dux[8], A. Herrmann[8], A. Kallenbach[8], R. McDermott[8], R. Neu[8], V. Rohde[8], E. Wolfrum[8] and the DIII-D and ASDEX-Upgrade teams

[1] Princeton Plasma Physics Lab., 100 Stellarator Rd, PO Box 241, Princeton, NJ 08543, USA

[2] General Atomics, PO Box 85608, San Diego, CA 92186, USA

[3] Massachusetts Institute of Technology, Cambridge, MA 02139, USA

[4] Lawrence Livermore National Laboratory, Livermore, CA 94550, USA

[5] University of California, San Diego, CA 92093, USA

[6] Oak Ridge National Laboratory, Oak Ridge, TN 37831, USA

[7] University of Tennessee Knoxville, Knoxville, TN 37996, USA

[8] Max-Planck-Institut für Plasmaphysik, EURATOM Association, Garching, 85748,Germany

Glow discharge boronization (GDB), i.e. chemical coating the plasma facing components with a B-rich layer [1], is a commonly-used method to pre-condition the plasma facing components of fusion devices. Although well-established, GDB entails handling hazardous gases (e.g. B_2D_6) and require interruptions of experimental operation, with possible evacuation of facilities. Furthermore, GDB is inapplicable to long pulse devices, in which the deposited coatings will significantly erode during a plasma discharge. Recent experiments carried out in the DIII-D [2] and ASDEX-Upgrade (AUG) [3] tokamaks, explored the possibility of generating boron coatings in "real-time," by injection of boron and boron enriched powders during tokamak operation. The experiments were enabled by a new impurity powder dropper designed to inject calibrated amounts of a wide range of impurity powders [4], which was recently installed and commissioned on both machines.

In DIII-D (graphite plasma facing components, PFCs), the experimental test of wall conditioning effect of B powder injection (BPI) was carried out as part of the DIII-D start-up operation, after a two-day machine vent in air for installation of in-vessel components. Approximately 40 plasma cleaning discharges preceded the B injection experiment to promote desorption of impurities (water, oxygen, nitrogen) and deuterium from the graphite PFCs, amounting to approximately 100 s of plasma operation. The experiment consisted in five consecutive lower single null plasma discharges with B powder injected in the current

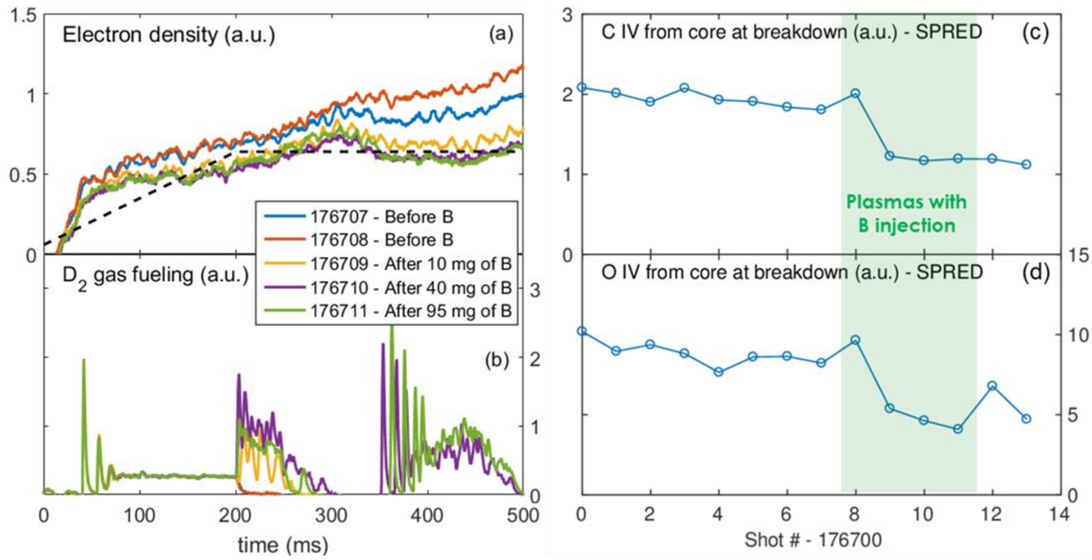

Figure 1. Left: electron density (a) and gas fueling (b) during I_p ramp for a series of consecutive shots, labeled by the cumulative amount of B injected prior to the shot execution. The dashed line represents the programmed target density. B injections begin with shot 176708 (red curve). Right: shot by shot evolution of the brightness of two intrinsic impurity lines at the discharge breakdown.

flat top phase for time intervals of 1-3 s, at rates 10-120 mg/s. Commercially available B powder was used, of particle size 40-100 um, isotopically enriched to >95% B^{11} (GDB employs natural B, with 19.8% B^{10}, 80.2% B^{11}). The B powder was injected through a vertical tube to reach the plasma crown at a speed of ~10 m/s after 1.7 m of nominal free fall. Estimates of ablation time suggest that particles of the injected size range ablate in the near scrape-off layer (SOL), i.e., close to the last closed flux surface (LCFS).

The Divertor Materials Evaluation System (DiMES) [5] sample manipulator was used to introduce a graphite sample flush with the divertor tiles, to obtain a quantitative evaluation of the wall coating effects. In these lower single null plasmas, the DiMES sample was exposed to the outboard SOL plasma at normalized poloidal flux ψ_N~1.05. DiMES was inserted before the first plasma with BPI and retracted two discharges after the last. In this case, post-mortem analysis provided information on the cumulative effects over multiple discharges.

A general reduction of wall fueling emerged from the time histories of density and gas fueling. In these discharges a D_2 fueling valve was activated according to a pre-programmed waveform up to t=200 ms, when the density feedback control was engaged. Figure 1(a,b) compare the evolution of the plasma density, in number of interferometer fringes, with the target value programmed in the control system. Before beginning of B injections, the experimental density exceeded the target, even after the gas valve was shut off by the feedback control at t=200 ms, providing a clear indication of fueling dominated by wall desorption. Conversely, after the first injection on B, the plasma density remained close to the

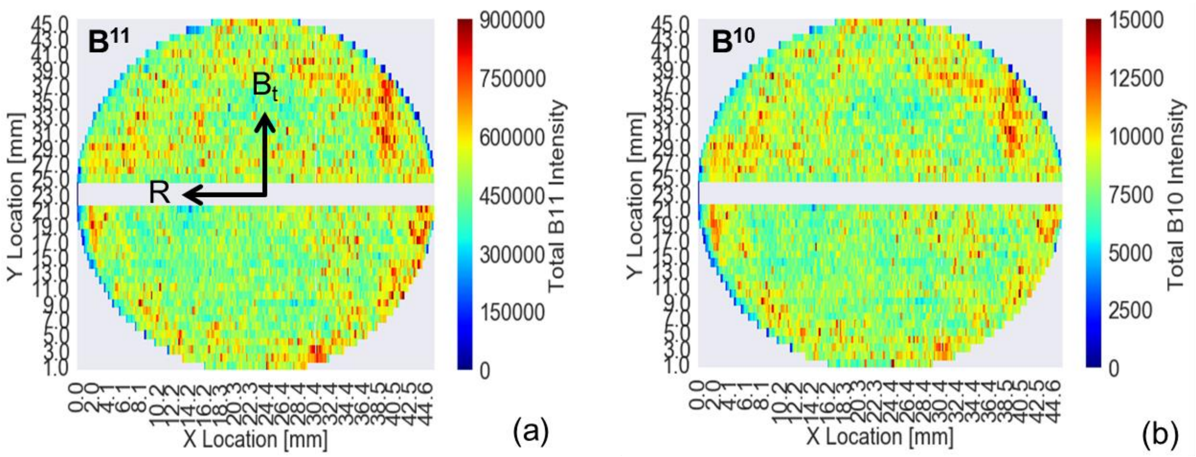

Figure 2. Map of intensity of B^{11} (a) and B^{10} (b) of DiMES sample surface measured with LAMS. The relative magnitude of the two measurements indicates a B^{11} isotope abundance ~98%.

request, with the gas valve opened by the feedback control to compensate for values lower than the request. It can also be seen that in subsequent shots, the similar values of L-mode density were obtained by applying consistently higher gas fueling. This clearly indicates the effect of a “pumping” wall in this early phase of the plasma discharge.

B injection was also observed to affect the impurity dynamics. Figure 1(c,d) show the shot-by-shot evolution of brightness of CIV and OIV lines measured by the vacuum-ultraviolet spectrometer SPRED at breakdown (t=0-100 ms), whose magnitude is monitored to assess the quality of wall conditions. A shaded region indicates the plasmas with B injection, carried out during the flat top starting from shot 176708. The data series show clear changes in trends correlating with the beginning of B injections. Notably, step-wise reductions in C and O emission were observed after injection of B powder, both reduced by a factor of 30-50%. Post-mortem analysis of the DiMES samples through Laser Ablation Mass Spectroscopy (LAMS) found layers of B associated with the powder injection. Figure 2 shows the map of B^{10} and B^{11} respectively, found with 2D LAMS analysis of the DiMES cap. Both isotopes were detected across the entire sample surfaces with signal well above noise level. Localized regions of higher signal emerge from a uniform background, with similar pattern for both species. As a consequence, the ratio between the measured intensity of B^{11}/B^{10} remains constant across the surface, with relative abundance of B^{11}~98%, indicating successful deposition of a new B-rich layer (i.e. not from redeposition of natural B) by BPI.

Wall conditioning improvement similar to boronization was also observed in AUG (tungsten PFCs) following injection of B and BN into H-mode discharges. Figure 3 shows the brightness of selected impurity lines, from the outer divertor and on the ICRF antenna limiter, measured in four plasma discharges as a function of the cumulative amount of B previously

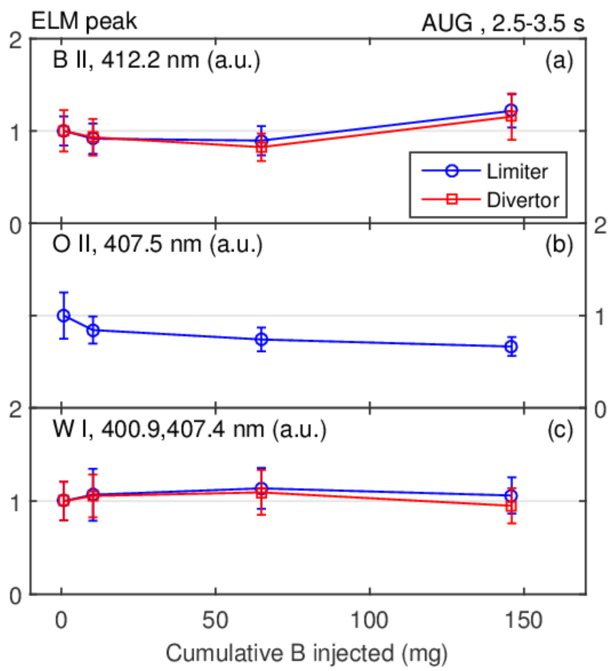

Figure 3. Normalized brightness of selected impurity lines measured from the limiter and divertor during ELM peaks. Data points are shown as a function of the cumulative B injected before the discharge execution.

injected in the machine. After an initial reduction, an increase of B II emission up to 25% is observed for cumulative amounts ~150 mg. At the same time, a decreasing trend is found for O II, monotonically decreasing to amplitudes ~30% smaller than the initial values. These observations are consistent with the growth of a B layer on the limiter acting as oxygen getter. A small increase of W emission by 10% is found up to 65 mg of B, with a tendency to roll-over for larger injected amounts ~150 mg. Overall, the results suggest that, by covering the W at the limiters, injected amounts of B larger than 100 mg are sufficient to cause appreciable wall conditioning effects.

The combined DIII-D and AUG dataset suggests that BPI during plasma operation could be used effectively to supplement the standard boronization and extend its beneficial effects by regenerating the coatings, in present-day and, potentially, next-step devices.

[1] O. I. Buzhinskij et al., Fusion Technol., vol. 32, no. 1, pp. 1–13, 1997.
[2] A. Bortolon et al., in Bull. Am. Phys. Soc., 2018, p. 63.
[3] A. Bortolon et al., Nucl. Mater. Energy, vol. 19, pp. 384–389, 2019.
[4] A. Nagy et al., Rev. Sci. Instrum., vol. 89, no. 10, p. 10K121, 2018.
[5] C. P. C. Wong et al., J. Nucl. Mater., vol. 196–198, pp. 71–75, 1992.

Work supported by the U.S. Department of Energy, Office of Science, Office of Fusion Energy Sciences, under Awards DE-FC02-04ER54698, DE-AC02-09CH11466, DE-SC0014264, DE-AC52-07NA27344, DE-SC0016318, DE-SC0019256, DE-AC05-00OR22725, DE-FG02-07ER54917.